

# 1 The interaction of CO<sub>2</sub> concentrations and water stress in 2 semi-arid areas causes diverging response in instantaneous 3 water use efficiency and carbon isotope composition

4 Na Zhao<sup>1</sup>, Ping Meng<sup>2</sup>, Yabing He<sup>1</sup>, Xinxiao Yu<sup>1\*</sup>

5 <sup>1</sup> College of soil and water conservation, Beijing Forestry University, Beijing 100083, P.R. China

6 <sup>2</sup> Research Institute of Forestry, Chinese Academy of Forestry 100091, Beijing, P.R. China

7 **Abstract.** In the context of global warming attributable to the increasing levels of CO<sub>2</sub>, severe drought  
8 can be anticipated in areas with chronic water shortages (semi-arid areas), which necessitates research  
9 on the interaction between elevated atmospheric concentrations of CO<sub>2</sub> and drought on plant  
10 photosynthetic discrimination. It is commonly surveyed that the <sup>13</sup>C fractionation derived from the  
11 CO<sub>2</sub> diffusion occurred from ambient air to stomatal sub-cavity, and little investigate the <sup>13</sup>C  
12 fractionation generated from the site of carboxylation to cytoplasm before sugars transportation  
13 outward the leaf, which may respond to the environmental conditions (i. e. CO<sub>2</sub> concentration and  
14 water stress) and their interactions. Therefore, saplings of species typical to a semi-arid area of  
15 Northern China that have similar growth status—*Platycladus orientalis* and *Quercus variabilis*—were  
16 selected and cultivated in growth chambers with orthogonal treatments (four CO<sub>2</sub> concentrations [CO<sub>2</sub>]  
17 × five soil volumetric water contents (SWC)). The δ<sup>13</sup>C of water-soluble compounds extracted from  
18 leaves of potted saplings was measured to determine the instantaneous water use efficiency (WUE<sub>cp</sub>)  
19 after cultivation. Instantaneous water use efficiency derived from gas exchange (WUE<sub>ge</sub>) was  
20 integrated to estimate differences in δ<sup>13</sup>C signal variation before leaf-exported translocation of primary  
21 assimilates. The WUE<sub>ge</sub> of the two saplings both decreased with increased soil moisture, and increased  
22 with elevated [CO<sub>2</sub>] at 35%–80% of Field Capacity (FC) by strengthening photosynthetic capacity and  
23 reducing transpiration. Differences in instantaneous water use efficiency (iWUE) according to distinct  
24 environmental changes differed between the species. The WUE<sub>ge</sub> of *P. orientalis* was significantly  
25 greater than that of *Q. variabilis*, while the opposite results were obtained in a comparison of the  
26 WUE<sub>cp</sub> of the two species. Total <sup>13</sup>C fractionation from the site of carboxylation to cytoplasm before  
27 sugars transportation (total <sup>13</sup>C fractionation) was clearly species-specific, as demonstrated in the  
28 interaction of [CO<sub>2</sub>] and SWC. Rising [CO<sub>2</sub>] coupled with moistened soil generated increasing  
29 disparities of δ<sup>13</sup>C between the water soluble compounds (δ<sup>13</sup>C<sub>WSC</sub>) and estimated by gas-exchange  
30 observation (δ<sup>13</sup>C<sub>obs</sub>) in *P. orientalis* with an amplitude of 0.0328‰–0.0472‰. Further, the  
31 differences between δ<sup>13</sup>C<sub>WSC</sub> and δ<sup>13</sup>C<sub>obs</sub> of *Q. variabilis* increased as CO<sub>2</sub> concentration increased  
32 and water stress alleviated (0.0384‰–0.0466‰). Fractionations from mesophyll conductance and  
33 post-photosynthesis both contributed to the total <sup>13</sup>C fractionation determined by two measurements  
34 (1.06%–24.94% and 75.30%–98.9% of total <sup>13</sup>C fractionation, respectively). Total <sup>13</sup>C fractionations  
35 were linearly dependent on g<sub>s</sub>, indicating post-carboxylation fractionation was attributed to  
36 environmental variation. Thus, cautious descriptions of the magnitude and environmental dependence  
37 of apparent post-carboxylation fractionation are worth our attention in photosynthetic fractionation.

38 **Key words:** Post-carboxylation fractionation; Carbon isotope fractionation; Elevated CO<sub>2</sub>

39 concentration; Soil volumetric water content; Instantaneous water use efficiency

## 40 1 Introduction

41 Since the onset of the industrial revolution, the atmospheric CO<sub>2</sub> concentration has increased at an  
42 annual rate of 0.4%, and is expected to increase further to 700 μmol·mol<sup>-1</sup>, together with more frequent  
43 periods of low water availability (IPCC, 2014). Increasing atmospheric CO<sub>2</sub> concentrations that trigger  
44 an ongoing greenhouse effect will not only lead to fluctuations in global patterns of precipitation, but  
45 also will amplify drought in arid regions, and lead to more frequent occurrences of extreme drought  
46 events in humid regions (Lobell et al., 2014). Accompanying the increasing concentration of CO<sub>2</sub>, the  
47 mean δ<sup>13</sup>C of atmospheric CO<sub>2</sub> is depleted by 0.02‰–0.03‰ year<sup>-1</sup> (data available from the  
48 CU-INSTAAR/NOAACMDL network for atmospheric CO<sub>2</sub>; <http://www.esrl.noaa.gov/gmd/>).

49 The carbon isotopic composition determined recently could respond more subtly to environmental  
50 changes and their influences on diffusion via plant physiology and metabolic processes (Gessler et al.,  
51 2014; Streit et al., 2013). While the depletion of δ<sup>13</sup>C<sub>CO<sub>2</sub></sub> has been shown in the atmosphere, variations  
52 in CO<sub>2</sub> concentration itself also might affect the δ<sup>13</sup>C of plant organs that, in turn, respond  
53 physiologically to climatic change (Gessler et al., 2014). The carbon discrimination (<sup>13</sup>Δ) of leaves  
54 could also provide timely feedback about the availability of soil moisture and the atmospheric vapor  
55 pressure deficit (Cemusak et al., 2012). Discrimination against <sup>13</sup>C in leaves relies mainly on  
56 environmental factors that affect the ratio of intercellular to ambient CO<sub>2</sub> concentration ( $C_i/C_a$ ) and  
57 Rubisco activities, even the mesophyll conductance derived from the difference of CO<sub>2</sub> concentrations  
58 between intercellular site and chloroplast (Farquhar et al., 1982; Cano et al., 2014). As changes in  
59 environmental conditions affect photosynthetic discrimination, they are expected to be recorded  
60 differentially in the δ<sup>13</sup>C of water-soluble organic matter (δ<sup>13</sup>C<sub>WSOM</sub>) of the different plant organs.  
61 Meanwhile, several processes during photosynthesis alter the δ<sup>13</sup>C of carbon transported within plants  
62 considerably. Carbon-fractionation during photosynthetic CO<sub>2</sub> fixation has been described and  
63 reviewed well elsewhere (Farquhar et al., 1982; Farquhar and Sharkey, 1982).

64 Post-photosynthetic fractionation is derived from equilibrium and kinetic isotopic effects, which  
65 determines isotopic differences between metabolites and intramolecular reaction positions, defined as  
66 “post-photosynthetic” or “post-carboxylation” fractionation (Jäggi et al., 2002; Badeck et al., 2005;  
67 Gessler et al., 2008). Post-carboxylation fractionation in plants includes the carbon discriminations that  
68 follow carboxylation of ribulose-1, 5-bisphosphate, and internal diffusion (RuBP, 27‰), as well as  
69 related transitory starch metabolism (Gessler et al., 2008; Gessler et al., 2014), fractionation in leaves,  
70 fractionation-associated phloem transport, the remobilization or storage of soluble carbohydrates, and  
71 starch metabolism fractionations in sink tissue (tree rings). In the synthesis of soluble sugars,  
72 <sup>13</sup>C-depletions of triose phosphates occur during exportation from the cytoplasm, and during  
73 production of fructose-1, 6-bisphosphate by aldolase in transitory starch synthesis (Rossmann  
74 et al., 1991; Gleixner and Schmidt, 1997). Synthesis of sugars before transportation to the twig is  
75 associated with the post-carboxylation fractionation generated in leaves. Although these are likely to  
76 play a role, what should be also considered is the CO<sub>2</sub> concentration in the chloroplast ( $C_c$ ), not in the  
77 intercellular space, as used in the simplified equation of the Farquhar’s model (Evans et al., 1986;  
78 Farquhar et al., 1989) is actually defined as carbon isotope discrimination (δ<sup>13</sup>C). Indeed, the difference  
79 between gas-exchange derived values and online measurements of δ<sup>13</sup>C has been widely used to  
80 estimate  $C_i-C_c$  and mesophyll conductance for CO<sub>2</sub> (Le Roux et al., 2001; Warren and Adams, 2006;  
81 Flexas et al., 2006; Evans et al., 2009; Flexas et al., 2012; Evans and von Caemmerer 2013). In this

82 regard, changes in mesophyll conductance could be partly responsible for the differences from two  
83 measurements, as it generally increases in the short term in response to elevated CO<sub>2</sub> (Flexas et al.,  
84 2014), whereas it tends to decrease under drought (Hommel et al., 2014; Th roux-Rancourt et al.,  
85 2014). Therefore, it is necessary to avoid confusion of carbon isotope discrimination derived from  
86 synthesis of soluble sugars or/and mesophyll conductance, and further, whether and what magnitude of  
87 these carbon fractionations are related to environmental variation have not yet been investigated.

88 The simultaneous isotopic analysis of leaves is a recent refinement in isotope studies that allows us  
89 to determine the temporal variation in isotopic fractionation (Rinne et al., 2016), and will help decipher  
90 environmental conditions more reliably. Newly assimilated carbohydrates can be extracted, and are  
91 defined as the water-soluble compounds (WSCs) in leaves (Brandes et al., 2006; Gessler et al., 2009),  
92 which also can be associated with an assimilation-weighted average of  $C_i/C_a$  (and  $C_d/C_a$ )  
93 photosynthesized over a period ranging from a few hours to 1-2 d (Pons et al., 2009). However, there is  
94 dispute whether the fractionation stemmed from post-carboxylation or/and mesophyll resistance may  
95 alter the stable signatures of leaf carbon and thence influence instantaneous water use efficiency  
96 (iWUE). In addition, the way in which the iWUE derived from these isotopic fractionations responds  
97 to different environmental factors, such as elevated [CO<sub>2</sub>] and/or soil water gradients, have not yet been  
98 observed.

99 Consequently, we investigated the  $\delta^{13}\text{C}$  of the fast-turnover carbohydrate pool in leaves from  
100 saplings of two trees typical in semi-arid areas of China—*Platycladus orientalis* and *Quercus*  
101 *variabilis*—together with simultaneous gas exchange measurements in control-environment of growth  
102 chambers (FH-230). Our goals are to differentiate the  $^{13}\text{C}$  fractionation from the site of carboxylation to  
103 cytoplasm before sugars transportation (total  $^{13}\text{C}$  fractionation) of *P. orientalis* and *Q. variabilis*, which  
104 were determined from the  $\delta^{13}\text{C}$  of water-soluble compounds and gas-exchange measurements, and then  
105 to discuss the potential causes for the observed divergence, estimate the contributions of  
106 post-photosynthetic and mesophyll resistance on these differences, and describe how these carbon  
107 isotopic fractionations respond to the interactive effects of elevated [CO<sub>2</sub>] and water stress.

## 108 2 Material and Methods

### 109 2.1 Study site and design

110 Saplings of *P. orientalis* and *Quercus variabilis* were selected as experimental material from the  
111 Capital Circle forest ecosystem station, a part of the Chinese Forest Ecosystem Research Network  
112 (CFERN, 40°03'45"N, 116°5'45"E) in Beijing, China. This region is populated by warm, temperate,  
113 deciduous, broad-leaved trees and mixed tree communities dominated by *Quercus variabilis* Bl. and  
114 *Platycladus orientalis* (L.) Franco, respectively. Saplings have similar ground diameters, heights, and  
115 growth statuses. The saplings were placed in pots 22 cm in diameter and 22 cm in height. Undisturbed  
116 soil samples were collected from the field in the research region, and the sieved soil (with all particles  
117 <10 mm removed) was placed in the pots. A single *P. orientalis* sapling was transplanted into each pot.  
118 The soil bulk density in the pots was maintained at 1.337–1.447 g cm<sup>-3</sup>. After one month of  
119 rejuvenation, the potted saplings were placed into chambers for cultivation.

120 The controlled experimental treatments were conducted in growth chambers (FH-230, Taiwan  
121 Hipoint Corporation, Kaohsiung City, Taiwan). To imitate the meteorological factors of the growth  
122 seasons in the research region, the daytime temperature in the chambers was set to 25 ± 0.5°C from  
123 07:00 to 17:00, and the night-time temperature was 18 ± 0.5°C from 17:00 to 07:00. Relative humidity

124 was maintained at 60% and 80% during the day and night, respectively. The light system was activated  
125 in the daytime and shut down at night. The average daytime light intensity was maintained at 200–240  
126  $\mu\text{mol m}^{-2} \text{s}^{-1}$ . CO<sub>2</sub> concentration was controlled by the central controlling system of the chambers  
127 (FH-230). Two growth chambers (A and B) were used in our study. Chamber A was switched in turn to  
128 maintain the CO<sub>2</sub> concentration of 400 ppm (during June 2–9, June 12–19, June 21–28, and July 2–9,  
129 2015, C<sub>400</sub>) and 500 ppm (during July 11–18, July 22–29, August 4–11, and August 15–22, 2015, C<sub>500</sub>).  
130 The other was adjusted to maintain the CO<sub>2</sub> concentration at 600 ppm (during June 2–9, June 12–19,  
131 June 21–28, and July 2–9, 2015, C<sub>600</sub>) and 800 ppm (during July 11–18, July 22–29, August 4–11, and  
132 August 15–22, 2015, C<sub>800</sub>). The target concentrations of CO<sub>2</sub> in the chambers were permitted the  
133 standard deviation of  $\pm 50$  ppm during cultivation. Thus, the gradient of four CO<sub>2</sub> concentrations in our  
134 study ( $400 \pm 50$  ppm,  $500 \pm 50$  ppm,  $600 \pm 50$  ppm, and  $800 \pm 50$  ppm) was formed. Detectors inside  
135 the chambers monitored and maintained the target concentrations of CO<sub>2</sub>.

136 We designed a device to water the potted plants automatically and avoid heterogeneity caused by  
137 interruptions in the watering process (Fig. 1). It consisted of the water storage tank, holder, controller,  
138 soil moisture sensors, and drip irrigation components. Prior to use, the water tank was filled with water,  
139 and the soil moisture sensor was inserted to a uniform depth in the soil. After connecting the controller  
140 to an AC power supply, specific soil water could be set. The soil volumetric water content (SWC) of  
141 the pot soil was monitored by the soil moisture sensors. Through the sensors, the irrigation device  
142 could determine whether to water or stop watering the plants. Two drip irrigation devices were  
143 installed in both chambers, respectively. Since the average Field Capacity (FC) of the pot soil was  
144 determined (30.70%), five levels of SWC were maintained before the orthogonal cultivations, as  
145 follows: 100% FC (or CK) (SWC approximately 27.63%–30.70%), 70%–80% of FC (SWC  
146 approximately 21.49%–24.56%), 60%–70% of FC (SWC approximately 18.42%–21.49%), 50%–60%  
147 of FC (SWC approximately 15.35%–18.42%), and 35%–45% of FC (SWC approximately 10.74%–  
148 13.81%). Each level of soil water was kept within the specific range thereafter by the irrigation device.

149 The Orthogonal tests were formed as: elevated CO<sub>2</sub> concentration gradient presented as 400 ppm,  
150 500 ppm, 600 ppm, and 800 ppm, combined with a soil-water gradient 35%–45% of FC, 50%–60% of  
151 FC, 60%–70% of FC, and 70%–80% of FC and 100% FC (CK). Undergoing the equilibrium  
152 circumstances of elevated CO<sub>2</sub> across the soil water gradients, the saplings were ready for investigation.  
153 Each orthogonal treatment continued for 7 days. Pots were rearranged periodically to minimize  
154 non-uniform illumination.

## 155 2.2 Foliar gas exchange measurement

156 Fully expanded primary annual leaves of the saplings were measured with a portable infrared gas  
157 photosynthesis system (LI-6400, Li-Cor, Lincoln, US) before and after the 7-day cultivation in the  
158 chambers. Two saplings per specie were replicated per treatment ([CO<sub>2</sub>] × water stress). For each  
159 sapling, four leaves were chosen and then four measurements were conducted on each leaf. The main  
160 photosynthetic parameters, such as net photosynthetic rate ( $P_n$ ) and transpiration rate ( $T_r$ ), were  
161 measured. Based on the theories proposed by Von Caemmerer and Farquhar (1981), stomatal  
162 conductance ( $g_s$ ) and intercellular CO<sub>2</sub> concentration ( $C_i$ ) were calculated by the Li-Cor software.  
163 Instantaneous water use efficiency via gas exchange ( $\text{WUE}_{ge}$ ) was calculated as the ratio of  $P_n$  to  $E$ .

## 164 2.3 Plant material collection and leaf water soluble compounds extraction

165 Recently-expanded, eight sun leaves per sapling were selected and frozen immediately in liquid  
166 nitrogen since the gas-exchange measurements accomplished. Two saplings per specie were chosen for

167 **each treatment.** A protocol adapted from Gessler et al. (2004) was used to extract the water-soluble  
 168 compounds (WSCs). All samples were ground to fine powders using mortars and liquid nitrogen. 50  
 169 mg of ground leaves and 100 mg PVPP (polyvinylpyrrolidone) were weighed, mixed evenly, and  
 170 incubated in 1mL double demineralized water for 60 min at 5°C in a centrifuge tube. Then, the tubes  
 171 were heated in 100°C water for 3 min. After they cooled to room temperature, the supernatant was  
 172 centrifuged at 12000 xg for 5 min and transferred 10 µL supernatant into tin capsule to be dried at 70°C.  
 173 Folded capsules were then ready for δ<sup>13</sup>C analysis of WSOM.

174 The samples of WSCs from leaves were combusted in an elemental analyzer (EuroEA, HEKAtech  
 175 GmbH, Wegberg, Germany) and analyzed in the mass spectrometer (DELTA<sup>plus</sup>XP, ThermoFinnigan).  
 176 Carbon isotope signatures are expressed in δ-notation in parts per thousand, relative to the international  
 177 Pee Dee Belemnite (PDB):

$$178 \quad \delta^{13}\text{C} = \left( \frac{R_{\text{sample}}}{R_{\text{standard}}} - 1 \right) \times 1000 \quad (1)$$

179 where δ<sup>13</sup>C is the heavy isotope and  $R_{\text{sample}}$  and  $R_{\text{standard}}$  refer to the isotope ratio between the  
 180 particular substance and the corresponding standard, respectively. The precision of the repeated  
 181 measurements was 0.1 ‰.

## 182 2.4 Isotopic calculation

### 183 2.4.1 <sup>13</sup>C fractionation from the site of carboxylation to cytoplasm before sugars transportation

184 Based on the linear model developed by Farquhar and Sharkey (1982), the isotope discrimination  
 185 factor, Δ, was calculated as:

$$186 \quad \Delta = \left( {}^{13}\text{C}_a - {}^{13}\text{C}_p \right) / \left( 1 + {}^{13}\text{C}_p \right) \quad (2)$$

187 where  ${}^{13}\text{C}_a$  is the isotope signature of ambient [CO<sub>2</sub>] in the chamber;  ${}^{13}\text{C}_p$  is the  ${}^{13}\text{C} : {}^{12}\text{C}$  of the  
 188 water-soluble compounds extracted from foliage. The  $C_i:C_a$  is determined by:

$$189 \quad C_i:C_a = (\Delta - a) / (b - a) \quad (3)$$

190 where  $C_i$  is the intercellular CO<sub>2</sub> concentration, and  $C_a$  is the ambient CO<sub>2</sub> concentration in the  
 191 chamber;  $a$  is the discrimination dependent on a fraction factor (4‰).  $b$  is the discrimination during  
 192 CO<sub>2</sub> fixation by ribulose 1,5- biphosphate carboxylase/oxygenase (Rubisco) and internal diffusion  
 193 (30‰). **Instantaneous water use efficiency by gas-exchange measurements (WUE<sub>ge</sub>)** is calculated as:

$$194 \quad \text{WUE}_{\text{ge}} = P_n : T_r = (C_a - C_i) / 1.6\Delta e \quad (4)$$

195 where  $P_n$  is the net carbon assimilation,  $T_r$  is the molar rate of transpiration, and 1.6 is the diffusion  
 196 ratio of stomatal conductance to water vapor to CO<sub>2</sub> in the chamber.  $\Delta e$  is the difference in water  
 197 vapor pressure between the intracellular in leaves and ambient air, which may be calculated as:

$$198 \quad \Delta e = e_{lf} - e_{atm} = 0.611 \times e^{17.502T / (240.97 + T)} \times (1 - \text{RH}) \quad (5)$$

199 where  $e_{lf}$  and  $e_{am}$  represent the extra- and **intra-cellular** water vapor pressure, respectively.  $T$  and RH is  
 200 temperature and relative humidity on leaf surface. **The instantaneous water use efficiency could be**  
 201 **determined by the δ<sup>13</sup>C<sub>WSC</sub> of leaves of two species, defined as WUE<sub>cp</sub>:**

$$202 \quad \text{WUE}_{\text{cp}} = \frac{P_n}{T_r} = (1 - \varphi) (C_a - C_i) / 1.6\Delta e = C_a (1 - \varphi) \left[ \frac{b - \delta^{13}\text{C}_a + (b+1)\delta^{13}\text{C}_{\text{WSC}}}{(b-a)(1 + \delta^{13}\text{C}_{\text{WSC}})} \right] / 1.6\Delta e \quad (6)$$

203  $\varphi$  is the ratio between carbohydrates consumed during respiration of the leaves and that of other  
 204 organs at night (0.3).  $\delta^{13}\text{C}_{\text{WSC}}$  is the carbon isotopic composition of water soluble compounds  
 205 extracted from leaves.

206 Then the  $^{13}\text{C}$  fractionation from the site of carboxylation to cytoplasm before sugars transportation  
 207 (total  $^{13}\text{C}$  fractionation) can be estimated by the observed  $\delta^{13}\text{C}$  of water soluble compounds from leaves  
 208 ( $\delta^{13}\text{C}_{\text{WSC}}$ ) and the modeled  $\delta^{13}\text{C}$  calculated from gas-exchange ( $\delta^{13}\text{C}_{\text{model}}$ ). The  $\delta^{13}\text{C}_{\text{model}}$  can be  
 209 calculated from  $\Delta_{\text{model}}$  from Eqn. (2). The  $\Delta_{\text{model}}$  can be determined by Eqns. (3 and 4) as:

$$210 \quad \Delta_{\text{model}} = (b - a) \left( 1 - \frac{1.6\Delta e^{\text{WUE}}_{ge}}{c_a} \right) + a \quad (7)$$

$$211 \quad \delta^{13}\text{C}_{\text{model}} = \frac{c_a - \Delta_{\text{model}}}{1 + \Delta_{\text{model}}} \quad (8)$$

$$212 \quad \text{Total } ^{13}\text{C fractionation} = \delta^{13}\text{C}_{\text{WSC}} - \delta^{13}\text{C}_{\text{model}} \quad (9)$$

#### 213 2.4.2 Methodology of calculating mesophyll conductance

214 Actually, the carbon isotope discrimination is generated from the relative contribution of diffusion  
 215 and carboxylation, reflected by the ratio of  $\text{CO}_2$  concentration at the site of carboxylation ( $C_c$ ) to that in  
 216 the ambient environment surrounding plants ( $C_a$ ). The carbon isotopic discrimination ( $\Delta$ ) could be  
 217 presented as (Farquhar et al. 1982):

$$218 \quad \Delta = a_b \frac{c_a - c_s}{c_a} + a \frac{c_s - c_i}{c_a} + (e_s + a_l) \frac{c_i - c_c}{c_a} + b \frac{c_c}{c_a} - \frac{eR_D + f\Gamma^*}{c_a} \quad (10)$$

219 where  $C_a, C_s, C_i$ , and  $C_c$  indicate the  $\text{CO}_2$  concentrations in the ambient environment, at the boundary  
 220 layer of leaf, in the intercellular air spaces before entrancing into solution, and at the sites of  
 221 carboxylation, respectively;  $a_b$  is the fractionation for the  $\text{CO}_2$  diffusion at the boundary layer (2.9‰);  
 222  $a$  is the fractionation occurring  $\text{CO}_2$  diffusion in still air (4‰);  $e_s$  is the discrimination of  $\text{CO}_2$   
 223 diffusion when  $\text{CO}_2$  enters in solution (1.1‰, at 25 °C);  $a_l$  is the fractionation derived from diffusion  
 224 in the liquid phase (0.7‰);  $b$  is the carboxylation discrimination in C3 plants (27‰);  $e$  and  $f$  are carbon  
 225 discrimination derived in dark respiration ( $R_D$ ) and photorespiration, respectively.  $k$  is the carboxylation  
 226 efficiency, and  $\Gamma^*$  is the  $\text{CO}_2$  compensation point in the absence of dark respiration (Brooks and  
 227 Farquhar, 1985).

228 When the gas in the cuvette could be well stirred during measurements of carbon isotopic  
 229 discrimination and gas exchange, the diffusion in the boundary layer could be neglected and Equation 7  
 230 could be shown:

$$231 \quad \Delta = a \frac{c_a - c_i}{c_a} + (e_s + a_l) \frac{c_i - c_c}{c_a} + b \frac{c_c}{c_a} - \frac{eR_D + f\Gamma^*}{c_a} \quad (11)$$

232 There is no agreement about the value of  $e$ , although recent measurements estimated it as 0-4‰. Value  
 233 of  $f$  has been estimated ranging at 8-12‰ (Gillon and Griffiths, 1997; Igamberdiev et al., 2004;  
 234 Lanigan et al., 2008). As the most direct factor, the value of  $b$  will influence the calculation for  $g_m$ , has  
 235 been thought to be close to 30‰ in higher plants (Guy et al., 1993).

236 The difference of  $\text{CO}_2$  concentration between the substomatal cavities and the chloroplast is omitted  
 237 while diffusion discrimination related with dark-respiration and photorespiration is also negligible, the  
 238 Equation 8 could be simplified as:

$$239 \quad \Delta_i = a + (b - a) \frac{c_i}{c_a} \quad (12)$$

240 Equation 12 presents the linear relationship between carbon discrimination and  $C_i/C_a$  that used  
 241 normally in carbon isotopic fractionation. That underlined the subsequent comparison between the  
 242 expected  $\Delta$  (originated from gas-exchange,  $\Delta_i$ ) and those actually measured ( $\Delta_{\text{obs}}$ ), which could  
 243 evaluate the magnitude of differences of  $\text{CO}_2$  concentration between the intercellular air and the sites of  
 244 carboxylation that generated by mesophyll resistance. Consequently,  $g_m$  can be estimated by

245 performing the  $\Delta_{obs}$  by isotope ratio mass spectrometry and expected  $\Delta_i$  from  $C_i/C_a$  by gas exchange  
 246 measurements.

247 Then subtract  $\Delta_{obs}$  of Equation 11 from  $\Delta_i$  calculated by Equation 12:

$$248 \quad \Delta_i - \Delta_{obs} = (b - e_s - a_l) \frac{C_i - C_c}{C_a} + \frac{\frac{eR_D + f\Gamma^*}{k} + \Gamma^*}{C_a} \quad (13)$$

249 and the net assimilation rate ( $A_n$ ) from the first Fick's law is presented by:

$$250 \quad A_n = g_m (C_i - C_c) \quad (14)$$

251 Substitute Equation 14 into Equation 13 we obtain:

$$252 \quad \Delta_i - \Delta_{obs} = (b - e_s - a_l) \frac{A_n}{g_m C_a} + \frac{\frac{eR_D + f\Gamma^*}{k} + \Gamma^*}{C_a} \quad (15)$$

$$253 \quad g_m = \frac{(b - e_s - a_l) \frac{A_n}{C_a}}{(\Delta_i - \Delta_{obs}) - \frac{eR_D/k + f\Gamma^*}{C_a}} \quad (16)$$

254 In calculation of  $g_m$ , the respiratory and photorespiratory terms could be ignored or be given the  
 255 specific constant values. Here,  $e$  and  $f$  are assumed to be zero or be cancelled out in the calculation of  
 256  $g_m$ .

257 Then Equation 16 can be transformed into:

$$258 \quad g_m = \frac{(b - e_s - a_l) \frac{A_n}{C_a}}{\Delta_i - \Delta_{obs}} \quad (17)$$

## 259 3 Results

### 260 3.1 Foliar gas exchange measurements

261 *P. orientalis* and *Q. variabilis* saplings were exposed to the orthogonal treatments. When SWC  
 262 increased,  $P_n$ ,  $g_s$  and  $T_r$  in *P. orientalis* and *Q. variabilis* peaked at 70%–80% of FC or/and FC (Fig. 2).  
 263 The  $C_i$  in *P. orientalis* rose as SWC increased, while it peaked at 60%–70% of FC and declined  
 264 thereafter with increased SWC in *Q. variabilis*. The capacity of carbon uptake and  $C_i$  were elevated  
 265 significantly by elevated  $[\text{CO}_2]$  at any given SWC for two species ( $p < 0.05$ ). Further, greater increasing  
 266 magnitudes of  $P_n$  in *P. orientalis* were found at 50%–70% of FC from  $C_{400}$  to  $C_{800}$ , which was at 35%–  
 267 45% of FC in *Q. variabilis*. As the water stress was alleviated (at 70%–80% of FC and FC), the  
 268 reduction of  $g_s$  in *P. orientalis* was more pronounced with elevated  $[\text{CO}_2]$  at a given SWC ( $p < 0.01$ ).  
 269 Nevertheless,  $g_s$  of *Q. variabilis* in  $C_{400}$ ,  $C_{500}$ , and  $C_{600}$  was significantly higher than that in  $C_{800}$  at  
 270 50%–80% of FC ( $p < 0.01$ ). Coordinated with  $g_s$ ,  $T_r$  of two species in  $C_{400}$  and  $C_{500}$  was significantly  
 271 higher than that in  $C_{600}$  and  $C_{800}$  except for 35%–60% of FC ( $p < 0.01$ , Figs. 2g and 2h). Larger  $P_n$ ,  $g_s$ ,  $C_i$   
 272 and  $T_r$  of *Q. variabilis* was significantly presented than that of *P. orientalis* ( $p < 0.01$ , Fig. 2).

### 273 3.2 $\delta^{13}\text{C}$ of water-soluble compounds in leaves

274 To observe the photosynthetic traits of the two saplings, the same leaf was frozen immediately and  
 275 the water-soluble compounds (WSCs) were extracted for all orthogonal treatments.  $\delta^{13}\text{C}_{\text{WSC}}$  ( $\delta^{13}\text{C}$  of  
 276 water-soluble compounds from leaves) of two species both increased as soil moisture improved (Figs.  
 277 3a and 3b,  $p < 0.01$ ). The average ( $\pm$  SD)  $\delta^{13}\text{C}_{\text{WSC}}$  of *P. orientalis* and *Q. variabilis* ranged from  $-27.44 \pm$   
 278  $0.155\text{‰}$  to  $-26.71 \pm 0.133\text{‰}$ , and from  $-27.96 \pm 0.129\text{‰}$  to  $-26.49 \pm 0.236\text{‰}$ , respectively. Similarly  
 279 with the photosynthetic capacity varying with increased SWC, average  $\delta^{13}\text{C}_{\text{WSC}}$  of two saplings reached  
 280 their maximums at 70%–80% of FC. Together with the gradual enrichment of  $[\text{CO}_2]$ , average  $\delta^{13}\text{C}_{\text{WSC}}$   
 281 in two species declined while  $[\text{CO}_2]$  exceeded 600 ppm ( $p < 0.01$ ). Except for  $C_{400}$  at 50%–100% of FC,  
 282  $\delta^{13}\text{C}_{\text{WSC}}$  of *P. orientalis* was significantly larger than that of *Q. variabilis* in any  $[\text{CO}_2] \times \text{SWC}$

283 treatment ( $p < 0.01$ , Fig. 3).

### 284 3.3 Estimations of $WUE_{ge}$ and $WUE_{cp}$

285 Instantaneous water use efficiency via gas exchange ( $WUE_{ge}$ ) is calculated as  $P_n$  divided by  $T_r$ .  
286 Figure 4a shows that **incremental** magnitudes of  $WUE_{ge}$  in *P. orientalis* under severe drought (i.e.,  
287 35%–45% of FC) were highest at any given  $[CO_2]$ , ranging from 90.70% to 564.65%.  $WUE_{ge}$  in *P.*  
288 *orientalis* reduced as SWC increased, while they increased remarkably as  $[CO_2]$  elevated. Compared to  
289 *P. orientalis*, trends of  $WUE_{ge}$  in *Q. variabilis* were promoted slightly at FC in  $C_{600}$  or  $C_{800}$  as soil  
290 moistened (Fig. 4b). The maximum of  $WUE_{ge}$  thus occurred at 35%–45% of FC in  $C_{800}$  among all  
291 orthogonal treatments for *P. orientalis*, as well as that for *Q. variabilis*. Further, elevated  $[CO_2]$   
292 enhanced the  $WUE_{ge}$  of *Q. variabilis* clearly at any SWC except that at 60%–80% of FC. Most saplings  
293 of *P. orientalis* had greater  $WUE_{ge}$  than did *Q. variabilis* between the same  $[CO_2] \times SWC$  treatments  
294 ( $p < 0.05$ ).

295 The instantaneous water use efficiency could be determined from Eqn. (6) by the  $\delta^{13}C_{WSC}$  of leaves  
296 of two species, defined as  $WUE_{cp}$ . As illustrated in Fig. 5a,  $WUE_{cp}$  of *P. orientalis* in  $C_{600}$  or  $C_{800}$   
297 climbed up as water stress alleviated beyond 50%–60% of FC, while the water threshold was 60%–70%  
298 of FC in  $C_{400}$  or  $C_{500}$ . *Q. variabilis* exhibited no uniform trend of  $WUE_{cp}$  with soil wetting (Fig. 5b).  
299 Except for  $C_{400}$ ,  $WUE_{cp}$  of *Q. variabilis* decreased abruptly at 50%–60% of FC, and then rose as soil  
300 moisture improved in  $C_{500}$ ,  $C_{600}$ , and  $C_{800}$ . In contrast to the findings about  $WUE_{ge}$  in two species,  
301  $WUE_{cp}$  of *Q. variabilis* was more pronounced than that of *P. orientalis* among all orthogonal  
302 treatments.

### 303 3.4 $^{13}C$ fractionation from the site of carboxylation to cytoplasm before sugars transportation

304 We evaluated the total  $^{13}C$  fractionation from the site of carboxylation to cytoplasm by gas exchange  
305 and  $\delta^{13}C$  of water-soluble compounds from leaf measurements (Table 1), which can retrace  $^{13}C$   
306 fractionation before carboxylation transport to the twig. Comparing  $\delta^{13}C_{WSC}$  with  $\delta^{13}C_{model}$  from  
307 Eqns. (4, 7 and 8), total  $^{13}C$  fractionation of *P. orientalis* ranged from 0.0328‰ to 0.0472‰, which  
308 was smaller than that of *Q. variabilis* (0.0384‰ to 0.0466‰). The total fractionations of *P. orientalis*  
309 were magnified with soil wetting especially that was increased by 21.30%–42.04% at 35%–80% of FC  
310 from  $C_{400}$  to  $C_{800}$ . Fractionation coefficients under  $C_{400}$  and  $C_{500}$  were amplified as SWC increased until  
311 50%–60% of FC in *Q. variabilis*, whereas it was increased at 50%–80% of FC and decreased at FC  
312 under  $C_{600}$  and  $C_{800}$ . Elevated  $[CO_2]$  enhanced the average fractionation effect of *P. orientalis*, while  
313 those of *Q. variabilis* declined sharply from  $C_{600}$  to  $C_{800}$ . Total  $^{13}C$  fractionation in *P. orientalis*  
314 increased faster than did those of *Q. variabilis* with increased soil moisture.

### 315 3.5 $g_m$ imposed on the interaction of $CO_2$ concentration and water stress

316 According to comparison between online leaf  $\delta^{13}C_{WSC}$  and the values of gas exchange measurements,  
317  $g_m$  over all treatments was presented in Fig. 6 (Eqns. 10–17). Significant increment trend of  $g_m$  was  
318 observed with water stress alleviated in *P. orientalis*, ranging from 0.0091–0.0690 mol  $CO_2$   $m^{-2}$   $s^{-1}$   
319 ( $p < 0.05$ ), which reached the maximums at FC under a given  $[CO_2]$ . Yet increases in  $g_m$  of *Q. variabilis*  
320 with increasing SWC become unremarkable except that under  $C_{400}$ . With  $CO_2$  concentration elevated,  
321  $g_m$  of two species was increased in different degrees. Comparing with *P. orientalis* under  $C_{400}$ ,  $g_m$  was  
322 increased gradiently and reached its maximum under  $C_{800}$  at 35%–60% of FC and FC ( $p < 0.05$ ),  
323 however, that was maximized under  $C_{600}$  ( $p < 0.05$ ) and slipped down under  $C_{800}$  at 60%–80% of FC.  
324 The maximum increment magnitude of  $g_m$  (8.2%–58.4%) occurred at  $C_{800}$  at any given SWC in *Q.*  
325 *variabilis*. It is evidently shown that  $g_m$  of *Q. variabilis* was larger than that of *P. orientalis* in the same

326 treatment.

### 327 **3.6 The contribution of post-carboxylation fractionation**

328 Here, the difference between  $\Delta_i$  and  $\Delta_{obs}$  presented the  $^{13}\text{C}$  fractionation derived from mesophyll  
329 conductance. So the post-photosynthetic fractionation after carboxylation can be calculated by  
330 subtracting the fractionation derived from mesophyll conductance from the total  $^{13}\text{C}$  fractionation that  
331 is generated from the site of carboxylation to cytoplasm before sugars transportation (Table 1). The  
332 fractionation from  $g_m$  had less contribution to total  $^{13}\text{C}$  fractionation than that from synthesis of sugars  
333 belong to post-carboxylation fractionation in any given treatment (Table 1). The contributions of  
334 fractionation from  $g_m$  with two species were illustrated different variations with soil water increasing,  
335 which declined at 50%–80% of FC and rose up at FC in *P. orientalis*, yet it was shown increasing with  
336 water stress alleviated at 50%–80% of FC and then decreased at FC in *Q. variabilis*. Nevertheless, the  
337 fractionations from synthesis of sugars in leaf and these contributions to total fractionation were all  
338 increased as soil moistened with two species. Considering the effects of enriched  $[\text{CO}_2]$  on  
339 fractionations of mesophyll conductance, the fractionation from mesophyll conductance reached its  
340 average peak under  $\text{C}_{600}$  in *P. orientalis*, which occurred under  $\text{C}_{800}$  with *Q. variabilis*.  
341 Post-photosynthetic fractionations were increased along with  $[\text{CO}_2]$  elevated in *P. orientalis*, which  
342 reached those maximums under  $\text{C}_{600}$  and then slipped down differing in degrees under  $\text{C}_{800}$ .

### 343 **3.7 Relationship between $g_s$ , $g_m$ and total $^{13}\text{C}$ fractionation**

344 Stoma is the conduit between the plant and atmosphere. Total  $^{13}\text{C}$  fractionation after carboxylation  
345 may be correlated with resistances derived from stomata and mesophyll cells. Here, we performed  
346 linear regressions between  $g_s/g_m$  and total  $^{13}\text{C}$  fractionation coefficient for *P. orientalis* and *Q. variabilis*,  
347 respectively (Fig. 7 and 8). It was apparent that total  $^{13}\text{C}$  fractionation coefficient was linearly  
348 dependent on the  $g_s$  ( $p < 0.05$ ), which controls the exchange of  $\text{CO}_2$  and  $\text{H}_2\text{O}$ , and responds to  
349 environmental variation. Subsequently, it was shown the linear relationships between  $g_m$  and the total  
350  $^{13}\text{C}$  fractionation coefficient, reflecting variation of  $\text{CO}_2$  concentration through the chloroplast was  
351 correlated with the carbon discrimination happened after photosynthesis in the leaf.

## 352 **4 Discussion**

### 353 **4.1 Photosynthetic traits**

354 The exchange of  $\text{CO}_2$  and water vapor via stomata is modulated in part by the soil or leaf water  
355 potential (Robredo et al., 2010). Saplings of *P. orientalis* reached their maximums of  $P_n$  and  $g_s$  at 70%–  
356 80% of FC under any  $[\text{CO}_2]$ . As SWC exceeded the water threshold, elevated  $\text{CO}_2$  caused a greater  
357 reduction in  $g_s$ , as has been reported for barley and wheat (Wall et al., 2011). Further, Maximal  $g_s$  of *Q.*  
358 *variabilis* in  $\text{C}_{400}$ ,  $\text{C}_{500}$ ,  $\text{C}_{600}$ , and  $\text{C}_{800}$  were generated successively as soil moisture increased, indicating  
359 that relative drought can stimulate the stomata which are more sensitive to environmental changes. In  
360 addition,  $C_i$  of *Q. variabilis* peaked at 60%–70% of FC and followed declines as soil moisture  
361 increased (Wall et al., 2006; Wall et al., 2011). This is interpreted as stomata having the tendency to  
362 maintain a constant  $C_i$  or  $C_i/C_a$  when ambient  $[\text{CO}_2]$  increases, which would determine the  $\text{CO}_2$  used  
363 directly in chloroplast (Yu et al., 2010). On the basis of theories (Farquhar and Sharkey, 1982) and  
364 common experimental technologies (Xu, 1997), this could be explained as the stomatal limitation.  
365 However,  $C_i$  of *P. orientalis* was increased considerably while SWC exceeded 70%–80% of FC, as  
366 found by Mielke et al. (2000). One factor that can account for that is plants close their stomata to

367 reduce intensive loss of water during the synthesis of organic matter, simultaneously decreasing the  
368 availability of CO<sub>2</sub> and generating respiration of organic matter (Robredo et al., 2007). Another  
369 explanation is the limited root volume in potted experiments may not be able to absorb sufficient water  
370 to support full growth of shoots (Leakey et al., 2009; Wall et al., 2011). In our study, further increasing  
371 [CO<sub>2</sub>] may cause nonstomatal limitation as SWC exceeding the threshold (70%–80% of FC), i.e.,  
372 accumulation of nonstructural carbohydrates in leaf tissue that induces mesophyll-based and/or  
373 biochemical-based transient inhibition of photosynthetic capacity (Farquhar and Sharkey, 1982). Xu  
374 and Zhou (2011) developed a five-level SWC gradient to examine the effect of water on the  
375 physiological characteristics of perennial *Leymus chinensis*, demonstrating that there was the soil water  
376 irrigation maximum below which the plant could manage itself to adjust changing environment.  
377 Miranda Apodaca et al. (2015) also concluded that, in suitable water conditions, elevated CO<sub>2</sub>  
378 augmented CO<sub>2</sub> assimilation of herbaceous plants.

379 The  $P_n$  of the two species increased with elevated [CO<sub>2</sub>] in our study, similarly with the results from  
380 C<sub>3</sub> woody plants (Kgope et al., 2010). Further, increasing [CO<sub>2</sub>] alleviated severe drought and heavy  
381 irrigation, which verifies that photosynthetic inhibition produced by water stress or excess may be  
382 mediated by increased [CO<sub>2</sub>] (Robredo et al., 2007; Robredo et al., 2010) and meliorate the adverse  
383 effects of drought stress by decreasing plant transpiration (Kirkham, 2016; Kadam et al., 2014;  
384 Miranda Apodaca et al., 2015; Tausz Posch et al., 2013).

#### 385 4.2 Differences between WUE<sub>ge</sub> and WUE<sub>cp</sub>

386 The increments of WUE<sub>ge</sub> in *P. orientalis* and *Q. variabilis* that resulted from the combination of an  
387 increase in  $P_n$  and decrease in  $g_s$ , followed by the reduction of  $T_r$  (Figs. 2a, 2g, 2b and 2h), also were  
388 demonstrated by Ainsworth and McGrath (2010). Combining  $P_n$  and  $T_r$  of two species in the same  
389 treatment, lower WUE<sub>ge</sub> in *Q. variabilis* is obtained due to its physiological and morphological traits,  
390 such as larger leaf area, rapid growth, and higher stomatal conductance than that of *P. orientalis*  
391 (Adiredjo et al., 2014). Medlyn et al. (2001) reported that the stomatal conductance of broadleaved  
392 species is more sensitive to elevated CO<sub>2</sub> concentrations than is that of conifers. Moreover, there has  
393 been no consensus on the patterns of iWUE with related soil water states at the leaf level, although  
394 some have discussed this topic (Yang et al., 2010). The WUE<sub>ge</sub> of *P. orientalis* and *Q. variabilis* was  
395 enhanced with water drying, as presented by Parker and Pallardy (1991), DeLucia and Heckathorn  
396 (1989), and Reich et al. (1989). Leakey (2009) also concluded that the WUE of plants in drought could  
397 be increased substantially, which was shown more clearly with elevated [CO<sub>2</sub>] in this study.

398 Bögelein et al. (2012) confirmed that WUE<sub>cp</sub> was more consistent with daily mean WUE<sub>ge</sub> than was  
399 WUE<sub>phloem</sub>. The WUE<sub>cp</sub> of two species demonstrated similar variation to those of  $\delta^{13}C_{WSC}$ , which  
400 differentiated with that of WUE<sub>ge</sub>. Pons et al. (2009) reviewed that  $\Delta$  in the leaf soluble sugar is  
401 coupled tightly with dynamics in the environment integrated over a period ranging from a few hours to  
402 1–2 d. WUE<sub>cp</sub> of our materials responded synthetically with SWC  $\times$  [CO<sub>2</sub>] gradients over cultivated  
403 days whereas WUE<sub>ge</sub> is characterized by the instantaneous state of plants to conditions. In addition,  
404 species-specific  $\delta^{13}C_{WSC}$  were observed in the same condition. Consequently, WUE<sub>cp</sub> and WUE<sub>ge</sub> have  
405 different variable curves according to treatments.

#### 406 4.3 The influence of mesophyll conductance on the fractionation after carboxylation

407 The consensus has been reached that the routine of CO<sub>2</sub> diffusion into photosynthetic site in plant  
408 includes two main procedures, which are CO<sub>2</sub> moving from ambient environment surrounding the leaf  
409 ( $C_a$ ) to the sub-stomatic cavities ( $C_i$ ) through stomata, and from there to the site of carboxylation within

410 the chloroplast stroma ( $C_c$ ) of leaf mesophyll. The latter diffusion is defined as mesophyll conductance  
411 ( $g_m$ ) (Flexas et al., 2008). Moreover,  $g_m$  has been identified to coordinate with environmental variables  
412 at the faster rate than that of stomatal conductance (Galmés et al., 2007; Tazoe et al., 2011; Flexas et al.,  
413 2007). During our 7-day cultivations of water stress  $\times$   $[\text{CO}_2]$ ,  $g_m$  increased and  $\text{WUE}_{\text{ge}}$  was decreased  
414 as soil moistened, which has been verified that  $g_m$  as the important factor could improve WUE under  
415 drought pretreatment (Han et al., 2016). There has been a dispute how  $g_m$  responds to fluctuation of  
416  $\text{CO}_2$  concentration. Terashima *et al.* (2006) have confirmed that  $\text{CO}_2$  permeable aquaporin, located in  
417 the plasma membrane and inner envelope of chloroplasts (Uehlein et al. 2008), could regulate the  
418 change of  $g_m$ . In our study, different species has specific-special  $g_m$  responding to the gradient of  $[\text{CO}_2]$ .  
419  $g_m$  of *P. orientalis* were significantly reduced by 9.08%-44.42% as  $[\text{CO}_2]$  rising from 600 to 800 ppm at  
420 60%-80% of FC, being similar to the results obtained by Flexas *et al.* (2007). Although larger  $g_m$  of *Q.*  
421 *variabilis* under  $C_{800}$  was observed, it made almost no difference.

422 Furthermore,  $g_m$  contributed to the  $^{13}\text{C}$  fractionation following the carboxylation while photosynthate  
423 has not been transported to the twigs of plant. The  $^{13}\text{C}$  fractionation of  $\text{CO}_2$  from air surrounding leaf to  
424 sub-stomatal cavity may be simply considered, whereas the fractionation induced by mesophyll  
425 conductance from sub-stomatic cavities to the site of carboxylation in the chloroplast cannot be  
426 neglected (Pons et al., 2009; Cano et al., 2014). As estimating the post-photosynthetic fractionation in  
427 leaf, carbon discrimination generated by mesophyll conductance must be subtracted from  $^{13}\text{C}$   
428 fractionation from the site of carboxylation to cytoplasm before sugars transportation (the difference  
429 between  $\delta^{13}\text{C}_{\text{WSC}}$  and  $\delta^{13}\text{C}_{\text{model}}$ ), which was closely associated with  $g_m$  (Fig 8,  $p < 0.05$ ). Similar  
430 variations of fractionation derived from  $g_m$  were presented with that of  $g_m$  under orthogonal tests on  
431 Table 1.

#### 432 4.4 Post-carboxylation fractionation generated before photosynthate leaving leaves

433 Photosynthesis, a biochemical and physiological process (Badeck et al., 2005), is characterized by  
434 discrimination against  $^{13}\text{C}$ , which leaves an isotopic signature in the photosynthetic apparatus. There is  
435 already a classic review of the carbon-fractionation in leaves (Farquhar et al., 1989) that covers the  
436 significant aspects of photosynthetic carbon isotope discrimination. The post-photosynthetic  
437 fractionation associated with the metabolic pathways of non-structural carbohydrates (NSC; defined  
438 here as soluble sugars + starch) within leaves, and fractionation during translocation, storage, and  
439 remobilization prior to tree ring formation remain unclear (Epron et al., 2012; Gessler et al., 2014;  
440 Rinne et al., 2016). The synthetic processes of sucrose and starch before transportation to the twig are  
441 within the domain of post-carboxylation fractionation generated in leaves. Hence, we hypothesized that  
442  $^{13}\text{C}$  fractionation might exist. When we finished the leaf gas exchange measurements, the leaf samples  
443 were collected immediately to determine the  $\delta^{13}\text{C}$  of water-soluble compounds ( $\delta^{13}\text{C}_{\text{WSC}}$ ). Presumably,  
444 the  $^{13}\text{C}$  fractionation generated in the synthetic processes of sucrose and starch was approximately  
445 contained within the  $^{13}\text{C}$  fractionation from the site of carboxylation to cytoplasm before sugars  
446 transportation as total  $^{13}\text{C}$  fractionation. When comparing  $\delta^{13}\text{C}_{\text{WSC}}$  with  $\delta^{13}\text{C}_{\text{obs}}$ , total fractionations  
447 of *P. orientalis* ranged from 0.0328‰ to 0.0472‰, less than that of *Q. variabilis* (from 0.0384‰ to  
448 0.0466‰). Then total  $^{13}\text{C}$  fractionation subtracted by fractionation derived from mesophyll  
449 conductance, post-photosynthetic fractionation occupied 75.30%-98.9% of total  $^{13}\text{C}$  fractionation.  
450 Recently, Gessler et al. (2004) reviewed the environmental drivers of variation in photosynthetic  
451 carbon isotope discrimination in terrestrial plants. The  $^{13}\text{C}$  fractionation of *P. orientalis* were enhanced  
452 by soil moistening, consistent with that of *Q. variabilis*, except at FC. The  $^{13}\text{C}$  isotope signature of *P.*  
453 *orientalis* was dampened by elevated  $[\text{CO}_2]$ . Yet,  $^{13}\text{C}$ -depletion was weakened in *Q. variabilis* in  $C_{600}$

454 and  $C_{800}$ . Linear regression between  $g_s$  and total  $^{13}\text{C}$  fractionation coefficient indicated that the  
455 post-carboxylation fractionation in leaves depended on the variation of  $g_s$  and stomata aperture  
456 correlated with environmental change.

## 457 5 Conclusions

458 Through orthogonal treatments of four  $[\text{CO}_2]$   $\times$  five SWC,  $\text{WUE}_{\text{cp}}$  calculated by  $\delta^{13}\text{C}$  of  
459 water-soluble compound and  $\text{WUE}_{\text{ge}}$  derived from simultaneous leaf gas exchange for leaves were  
460 estimated to differentiate the  $\delta^{13}\text{C}$  signal variation before leaf-exported translocation of primary  
461 assimilates. The influence of mesophyll conductance on the difference of  $^{13}\text{C}$  fractionation between the  
462 sub-stomatic cavities and the ambient environment need to be considered, while testing the hypothesis  
463 that the post-carboxylation will contribute to the  $^{13}\text{C}$  fractionation from the site of carboxylation to  
464 cytoplasm before sugars transportation. In response to the interactive effects of  $[\text{CO}_2]$  and SWC,  
465  $\text{WUE}_{\text{ge}}$  of the two species of saplings both decreased with soil moistening, and increased with elevated  
466  $[\text{CO}_2]$  at 35%–80% of FC. We concluded that relative soil drying, coupled with elevated  $[\text{CO}_2]$ , could  
467 improve  $\text{WUE}_{\text{ge}}$  by strengthening photosynthetic capacity and reducing transpiration.  $\text{WUE}_{\text{ge}}$  of *P.*  
468 *orientalis* was significantly greater than was that of *Q. variabilis*, while the opposite was the case for  
469  $\text{WUE}_{\text{cp}}$  in two species. Mesophyll conductance and post-photosynthesis were manifested both  
470 contributing to the  $^{13}\text{C}$  fractionation from the site of carboxylation to cytoplasm before sugars  
471 transportation determined by gas exchange and carbon isotopic measurements. Rising  $[\text{CO}_2]$  and/or soil  
472 moistening generated increasing disparities between  $\delta^{13}\text{C}_{\text{WSC}}$  and  $\delta^{13}\text{C}_{\text{model}}$  in *P. orientalis*;  
473 nevertheless, the differences between  $\delta^{13}\text{C}_{\text{WSC}}$  and  $\delta^{13}\text{C}_{\text{model}}$  in *Q. variabilis* increased as  $[\text{CO}_2]$   
474 being less than 600 ppm and/or water stress was alleviated. Total  $^{13}\text{C}$  fractionation in leaf was linearly  
475 dependent on  $g_s$ . With respect to carbon fractionation in post-carboxylation and transportation  
476 processes, we cannot neglect that the instantaneous water use efficiency derived from the synthesis of  
477 sucrose and starch were influenced inevitably by environmental changes. Thus, cautious descriptions of  
478 the magnitude and environmental dependence of apparent post-carboxylation fractionation are worth  
479 our attention in photosynthetic fractionation.

## 480 References

- 481 Adiredjo, A. L., Navaud, O., Lamaze, T., and Grieu, P.: Leaf carbon isotope discrimination as an  
482 accurate indicator of water use efficiency in sunflower genotypes subjected to five stable soil  
483 water contents, *J Agron. Crop Sci.*, 200, 416–424, 2014.
- 484 Ainsworth, E. A. and McGrath, J. M.: Direct effects of rising atmospheric carbon dioxide and ozone on  
485 crop yields, *Climate Change and Food Security*, Springer, 109–130, 2010.
- 486 Badeck, F. W., Tcherkez, G., Eacute, N. S. S., Piel, C. E. M., and Ghashghaie, J.: Post-photosynthetic  
487 fractionation of stable carbon isotopes between plant organ – a widespread phenomenon, *Rapid*  
488 *Commun. Mass S.*, 19, 1381–1391, 2005.
- 489 Bögelein, R., Hassdenteufel, M., Thomas, F. M., and Werner, W.: Comparison of leaf gas exchange  
490 and stable isotope signature of water-soluble compounds along canopy gradients of co-occurring  
491 Douglas-fir and European beech, *Plant Cell Environ.*, 35, 1245–1257, 2012.
- 492 Brandes, E., Kodama, N., Whittaker, K., Weston, C., Rennenberg, H., Keitel, C., Adams, M. A., and  
493 Gessler, A.: Short-term variation in the isotopic composition of organic matter allocated from the  
494 leaves to the stem of *Pinus sylvestris*: effects of photosynthetic and postphotosynthetic carbon

495 isotope fractionation, *Global Change Biol.*, 12, 1922–1939, 2006.

496 Brooks, A. and Farquhar, G. D.: Effect of temperature on the CO<sub>2</sub>/O<sub>2</sub> specificity of  
 497 ribulose-1,5-bisphosphate carboxylase/oxygenase and the rate of respiration in the light, *Planta*,  
 498 165, 397–406, 1985.

499 Brugnoli E, Farquhar GD. 2000. Photosynthetic fractionation of carbon isotopes. In: Leegood RC,  
 500 Sharkey TD, von Caemmerer S. eds. *Photosynthesis: physiology and metabolism. Advances in*  
 501 *photosynthesis*. Dordrecht, The Netherlands: Kluwer Academic Publishers, 399–434.

502 Cano, F. J., López, R., and Warren, C. R.: Implications of the mesophyll conductance to CO<sub>2</sub> for  
 503 photosynthesis and water-use efficiency during long-term water stress and recovery in two  
 504 contrasting *Eucalyptus* species, *Plant Cell Environ.*, 37, 2470–2490, 2014.

505 Cernusak, L. A., Ubierna, N., Winter, K., Holtum, J. A. M., Marshall, J. D., and Farquhar, G. D.:  
 506 Environmental and physiological determinants of carbon isotope discrimination in terrestrial  
 507 plants, *New Phytologist*, 200, 950–965, 2013.

508 DeLucia, E. H. and Heckathorn, S. A.: The effect of soil drought on water-use efficiency in a  
 509 contrasting Great Basin desert and Sierran montane species, *Plant Cell Environ.*, 12, 935–940,  
 510 1989.

511 Epron, D., Nouvellon, Y., and Ryan, M. G.: Introduction to the invited issue on carbon allocation of  
 512 trees and forests, *Tree physiol.*, 32, 639–643, 2012.

513 Evans, J. R., Kaldenhoff, R., Genty, B., and Terashima, I.: Resistances along the CO<sub>2</sub> diffusion  
 514 pathway inside leaves, *J. Exp. Bot.*, 60, 2235–2248, 2009.

515 Evans, J. R., Sharkey, T. D., Berry, J. A., and Farquhar, G. D.: Carbon isotope discrimination measured  
 516 concurrently with gas-exchange to investigate CO<sub>2</sub> diffusion in leaves of higher-plants, *Funct.*  
 517 *Plant Biol.*, 13, 281–292, 1986.

518 Evans, J. R. and von Caemmerer, S.: Temperature response of carbon isotope discrimination and  
 519 mesophyll conductance in tobacco, *Plant Cell Environ.*, 36, 745–756, 2013.

520 Farquhar, G. D., Ehleringer, J. R., and Hubick, K. T.: Carbon isotope discrimination and  
 521 photosynthesis, *Ann. Rev. Plant Physiol.*, 40, 503–537, 1989.

522 Farquhar, G. D., O'Leary, M. H., and Berry, J. A.: On the relationship between carbon isotope  
 523 discrimination and the intercellular carbon dioxide concentration in leaves, *Funct. Plant Biol.*, 9,  
 524 121–137, 1982.

525 Farquhar, G. D. and Sharkey, T. D.: Stomatal conductance and photosynthesis, *Ann. Rev. Plant*  
 526 *Physiol.*, 33, 317–345, 1982.

527 Flexas, J., Barbour, M. M., Brendel, O., Cabrera, H. M., Carriqui M., Díaz-Espejo, A., Douthe, C.,  
 528 Dreyer, E., Ferrio, J. P., Gago, J., Gallé A., Galmés, J., Kodama, N., Medrano, H., Niinemets, Ü.,  
 529 Peguero-Pina, J. J., Pou, A., Ribas-Carbó, M., Tomás, M., Tosens, T., and Warren, C. R.:  
 530 Mesophyll diffusion conductance to CO<sub>2</sub>: An unappreciated central player in photosynthesis, *Plant*  
 531 *Science*, 193–194, 70–84, 2012.

532 Flexas, J., Carriqui M., Coopman, R. E., Gago, J., Galmés, J., Martorell, S., Morales, F., and  
 533 Díaz-Espejo, A.: Stomatal and mesophyll conductances to CO<sub>2</sub> in different plant groups:  
 534 Underrated factors for predicting leaf photosynthesis responses to climate change? *Plant Science*,  
 535 226, 41–48, 2014.

536 Flexas, J., Díaz-Espejo, A., Galmés, J., Kaldenhoff, R., Medano, H., and Ribas-Carbo, M.: Rapid  
 537 variations of mesophyll conductance in response to changes in CO<sub>2</sub> concentration around leaves,  
 538 *Plant Cell Environ.*, 30, 1284–1298, 2007.

539 Flexas, J., Ribas-Carbó, M., Diaz-Espejo, A., Galmés, J., and Medrano, H.: Mesophyll conductance to  
540 CO<sub>2</sub>: current knowledge and future prospects, *Plant Cell Environ.*, 31, 602–621, 2008.

541 Flexas, J., Ribas-Carbó, M., Hanson, D.T., Bota, J., Otto, B., Cifre, J., McDowell, N., Medrano, H., and  
542 Kaldenhoff, R.: Tobacco aquaporin NtAQP1 is involved in mesophyll conductance to CO<sub>2</sub> *in vivo*,  
543 *Plant J.*, 48, 427–439, 2006.

544 Galmés, J., Medrano, H., and Flexas, J.: Photosynthetic limitations in response to water stress and  
545 recovery in Mediterranean plants with different growth forms, *New Phytol.*, 175, 81–93. 2007.

546 Gessler, A., Brandes, E., Buchmann, N., Helle, G., Rennenberg, H., and Barnard, R. L.: Tracing carbon  
547 and oxygen isotope signals from newly assimilated sugars in the leaves to the tree-ring archive,  
548 *Plant Cell Environ.*, 32, 780–795, 2009.

549 Gessler, A., Ferrio, J. P., Hommel, R., Treydte, K., Werner, R. A., and Monson, R. K.: Stable isotopes  
550 in tree rings: towards a mechanistic understanding of isotope fractionation and mixing processes  
551 from the leaves to the wood, *Tree Physiol.*, 34, 796–818, 2014.

552 Gessler, A., Rennenberg, H., and Keitel, C.: Stable isotope composition of organic compounds  
553 transported in the phloem of European beech-evaluation of different methods of phloem sap  
554 collection and assessment of gradients in carbon isotope composition during leaf-to-stem transport,  
555 *Plant Biology*, 6, 721–729, 2004.

556 Gessler, A., Tcherkez, G., Peuke, A. D., Ghashghaie, J., and Farquhar, G. D.: Experimental evidence  
557 for diel variations of the carbon isotope composition in leaf, stem and phloem sap organic matter  
558 in *Ricinus communis*, *Plant Cell Environ.*, 31, 941–953, 2008.

559 Gillon, J. S., Griffiths, H.: The influence of (photo)respiration on carbon isotope discrimination in  
560 plants. *Plant Cell Environ.*, 20, 1217–1230, 1997.

561 Gleixner, G. and Schmidt, H.: Carbon isotope effects on the fructose-1, 6-bisphosphate aldolase  
562 reaction, origin for non-statistical <sup>13</sup>C distributions in carbohydrates, *J. Biol. Chem.*, 272, 5382–  
563 5387, 1997.

564 Guy, R. D., Fogel, M. L., and Berry, J. A.: Photosynthetic fractionation of the stable isotopes of oxygen  
565 and carbon, *Plant Physiol.*, 101, 37–47, 1993.

566 Han, J. M., Meng, H. F., Wang, S. Y., Jiang, C. D., Liu, F., Zhang, W. F., and Zhang, Y. L.: Variability  
567 of mesophyll conductance and its relationship with water use efficiency in cotton leaves under  
568 drought pretreatment, *J. Plant Physiol.*, 194, 61–71, 2016.

569 Hommel, R., Siegwolf, R., Saurer, M., Farquhar, G. D., Kayler, Z., Ferrio, J. P., and Gessler, A.:  
570 Drought response of mesophyll conductance in forest understory species-impacts on water-use  
571 efficiency and interactions with leaf water movement, *Physiol. Plantarum*, 152, 98–114, 2014.

572 Igamberdiev, A. U., Mikkelsen, T. N., Ambus, P., Bauwe, H., and Lea, P. J.: Photorespiration  
573 contributes to stomatal regulation and carbon isotope fractionation: a study with barley, potato and  
574 *Arabidopsis* plants deficient in glycine decarboxylase, *Photosynth. Res.*, 81, 139–152, 2004.

575 IPCC: Summary for policymakers, in: *Climate Change 2014, Mitigation of Climate Change*,  
576 contribution of Working Group III to the Fifth Assessment Report of the Intergovernmental Panel  
577 on Climate Change, edited by: Edenhofer, O., Pichs-Madruga, R., Sokona, Y., Farahani, E.,  
578 Kadner, S., Seyboth, K., Adler, A., Baum, I., Brunner, S., Eickemeier, P., Kriemann, B.,  
579 Savolainen, J., Schlomer, S., von Stechow, C., Zwickel, T., and Minx, J. C., Cambridge  
580 University Press, Cambridge, UK and New York, NY, USA, 1–30, 2014.

581 Jäggi, M., Saurer, M., Fuhrer, J., and Siegwolf, R.: The relationship between the stable carbon isotope  
582 composition of needle bulk material, starch, and tree rings in *Picea abies*, *Oecologia*, 131, 325–

583 332, 2002.

584 Kadam, N. N., Xiao, G., Melgar, R. J., Bahuguna, R. N., Quinones, C., Tamilselvan, A., Prasad, P. V.  
585 V., and Jagadish, K. S. V.: Chapter three-agronomic and physiological responses to high  
586 temperature, drought, and elevated CO<sub>2</sub> interactions in cereals, *Adv. Agron.*, 127, 111–156, 2014.

587 Kgope, B. S., Bond, W. J., and Midgley, G. F.: Growth responses of African savanna trees implicate  
588 atmospheric [CO<sub>2</sub>] as a driver of past and current changes in savanna tree cover, *Austral Ecol.*, 35,  
589 451–463, 2010.

590 Kirkham, M. B.: Elevated carbon dioxide: impacts on soil and plant water relations, CRC Press,  
591 London, New York, 2016.

592 Kodama, N., Barnard, R. L., Salmon, Y., Weston, C., Ferrio, J. P., Holst, J., Werner, R. A., Saurer, M.,  
593 Rennenberg, H., and Buchmann, N.: Temporal dynamics of the carbon isotope composition in a  
594 *Pinus sylvestris* stand: from newly assimilated organic carbon to respired carbon dioxide,  
595 *Oecologia*, 156, 737–750, 2008.

596 Lanigan, G. J., Betson, N., Griffiths, H., and Seibt, U.: Carbon isotope fractionation during  
597 photorespiration and carboxylation in *Senecio*, *Plant Physiol.*, 148, 2013–2020, 2008.

598 Le Roux, X., Bariac, T., Sinoquet H., Genty, B., Piel, C., Mariotti, A., Girardin, C., and Richard, P.:  
599 Spatial distribution of leaf water-use efficiency and carbon isotope discrimination within an  
600 isolated tree crown, *Plant Cell Environ.*, 24, 1021–1032, 2001.

601 Leakey, A. D.: Rising atmospheric carbon dioxide concentration and the future of C4 crops for food  
602 and fuel, *Proceedings of the Royal Society of London B: Biological Sciences*, 276, 1517–2008,  
603 2009.

604 Leakey, A. D., Ainsworth, E. A., Bernacchi, C. J., Rogers, A., Long, S. P., and Ort, D. R.: Elevated  
605 CO<sub>2</sub> effects on plant carbon, nitrogen, and water relations: six important lessons from FACE, *J.*  
606 *Exp. Bot.*, 60, 2859–2876, 2009.

607 Lobell, D. B., Roberts, M. J., Schlenker, W., Braun, N., Little, B. B., Rejesus, R. M., and Hammer, G.  
608 L.: Greater sensitivity to drought accompanies maize yield increase in the US Midwest, *Science*,  
609 344, 516–519, 2014.

610 Medlyn, B. E., Barton, C. V. M., Broadmeadow, M. S. J., Ceulemans, R., Angelis, P. D., Forstreuter,  
611 M., Freeman, M., Jackson, S. B., Kellomäki, S., and Laitat, E.: Stomatal conductance of forest  
612 species after long-term exposure to elevated CO<sub>2</sub> concentration: a synthesis, *New Phytol.*, 149,  
613 247–264, 2001.

614 Mielke, M. S., Oliva, M. A., de Barros, N. F., Penchel, R. M., Martinez, C. A., Da Fonseca, S., and de  
615 Almeida, A. C.: Leaf gas exchange in a clonal eucalypt plantation as related to soil moisture, leaf  
616 water potential and microclimate variables, *Trees*, 14, 263–270, 2000.

617 Miranda Apodaca, J., Pérez López, U., Lacuesta, M., Mena Petite, A., and Muñoz Rueda, A.: The type  
618 of competition modulates the ecophysiological response of grassland species to elevated CO<sub>2</sub> and  
619 drought, *Plant Biolog.*, 17, 298–310, 2015.

620 Parker, W. C. and Pallardy, S. G.: Gas exchange during a soil drying cycle in seedlings of four black  
621 walnut (*Juglans nigra* L.) Families, *Tree physiol.*, 9, 339–348, 1991.

622 Pons, T. L., Flexas, J., von Caemmerer, S., Evans, J. R., Genty, B., Ribas-Carbo, M., and Brugnoli, E.:  
623 Estimating mesophyll conductance to CO<sub>2</sub>: methodology, potential errors, and recommendations,  
624 *J. Exp. Bot.*, 8, 1–18, 2009.

625 Reich, P. B., Walters, M. B., and Tabone, T. J.: Response of *Ulmus americana* seedlings to varying  
626 nitrogen and water status. 2 Water and nitrogen use efficiency in photosynthesis, *Tree Physiol.*, 5,

627 173–184, 1989.

628 Rinne, K. T., Saurer, M., Kirdeyanov, A. V., Bryukhanova, M. V., Prokushkin, A. S., Churakova  
629 Sidorova, O. V., and Siegwolf, R. T.: Examining the response of larch needle carbohydrates to  
630 climate using compound-specific  $\delta^{13}\text{C}$  and concentration analyses, EGU General Assembly  
631 Conference, 1814949R, 2016.

632 Robredo, A., Pérez-López, U., de la Maza, H. S., González-Moro, B., Lacuesta, M., Mena-Petite A.,  
633 and Muñoz-Rueda, A.: Elevated  $\text{CO}_2$  alleviates the impact of drought on barley improving water  
634 status by lowering stomatal conductance and delaying its effects on photosynthesis, *Environ. Exp.*  
635 *Bot.*, 59, 252–263, 2007.

636 Robredo, A., Pérez-López, U., Lacuesta, M., Mena-Petite, A., and Muñoz-Rueda, A.: Influence of  
637 water stress on photosynthetic characteristics in barley plants under ambient and elevated  $\text{CO}_2$   
638 concentrations, *Biologia. Plantarum*, 54, 285–292, 2010.

639 Rossmann, A., Butzenlechner, M., and Schmidt, H.: Evidence for a nonstatistical carbon isotope  
640 distribution in natural glucose, *Plant Physiol.*, 96, 609–614, 1991.

641 Streit, K., Rinne, K. T., Hagedorn, F., Dawes, M. A., Saurer, M., Hoch, G., Werner, R. A., Buchmann,  
642 N., and Siegwolf, R. T. W.: Tracing fresh assimilates through *Larix decidua* exposed to elevated  
643  $\text{CO}_2$  and soil warming at the alpine treeline using compound-specific stable isotope analysis, *New*  
644 *Phytol.*, 197, 838–849, 2013.

645 Tausz Posch, S., Norton, R. M., Seneweera, S., Fitzgerald, G. J., and Tausz, M.: Will intra-specific  
646 differences in transpiration efficiency in wheat be maintained in a high  $\text{CO}_2$  world? A FACE study,  
647 *Physiol. Plantarum*, 148, 232–245, 2013.

648 Tazoe, Y., von Caemmerer, S., Estavillo, G. M., and Evans, J. R.: Using tunable diode laser  
649 spectroscopy to measure carbon isotope discrimination and mesophyll conductance to  $\text{CO}_2$   
650 diffusion dynamically at different  $\text{CO}_2$  concentrations, *Plant Cell Environ.*, 34, 580–591, 2011.

651 Terashima, I., Hanba, Y.T., Tazoe, Y., Vyas, P., and Yano, S.: Irradiance and phenotype: comparative  
652 eco-development of sun and shade leaves in relation to photosynthetic  $\text{CO}_2$  diffusion, *J. Exp. Bot.*,  
653 57, 343–354, 2006.

654 Théroux-Rancourt, G., Éthier, G., and Pepin, S.: Threshold response of mesophyll  $\text{CO}_2$  conductance to  
655 leaf hydraulics in highly transpiring hybrid poplar clones exposed to soil drying, *J. Exp. Bot.*, 65,  
656 741–753, 2014.

657 Uehlein, N., Otto, B., Hanson, D. T., Fischer, M., McDowell, N., and Kaldenhoff, R.: Function of  
658 *Nicotiana tabacum* aquaporins as chloroplast gas pores challenges the concept of membrane  $\text{CO}_2$   
659 permeability, *Plant Cell*, 20, 648–657, 2008.

660 Von Caemmerer, S. V. and Farquhar, G. D.: Some relationships between the biochemistry of  
661 photosynthesis and the gas exchange of leaves, *Planta*, 153, 376–387, 1981.

662 Wall, G. W., Garcia, R. L., Kimball, B. A., Hunsaker, D. J., Pinter, P. J., Long, S. P., Osborne, C. P.,  
663 Hendrix, D. L., Wechsung, F., and Wechsung, G.: Interactive effects of elevated carbon dioxide  
664 and drought on wheat, *Agron. J.*, 98, 354–381, 2006.

665 Wall, G. W., Garcia, R. L., Wechsung, F., and Kimball, B. A.: Elevated atmospheric  $\text{CO}_2$  and drought  
666 effects on leaf gas exchange properties of barley, *Agr. Ecosyst. Environ.*, 144, 390–404, 2011.

667 Warren, C. R. and Adams, M. A.: Internal conductance does not scale with photosynthetic capacity:  
668 implications for carbon isotope discrimination and the economics of water and nitrogen use in  
669 photosynthesis, *Plant Cell Environ.*, 29, 192–201, 2006.

670 Xu, D. Q.: Some problems in stomatal limitation analysis of photosynthesis, *Plant Physiol. J.*, 33, 241–

671 244, 1997.  
672 Xu, Z. and Zhou, G.: Responses of photosynthetic capacity to soil moisture gradient in perennial  
673 rhizome grass and perennial bunchgrass, *BMC Plant Boil.*, 11, 21, 2011.  
674 Yang, B., Pallardy, S. G., Meyers, T. P., GU, L. H., Hanson, P. J., Wullschleger, S. D., Heuer, M.,  
675 Hosman, K. P., Riggs, J. S., and Sluss D. W.: Environmental controls on water use efficiency  
676 during severe drought in an Ozark Forest in Missouri, USA, *Global Change Biol.*, 16, 2252–2271,  
677 2010.  
678 Yu, G., Wang, Q., and Mi, N.: *Ecophysiology of plant photosynthesis, transpiration, and water use*,  
679 Science Press, Beijing, China, 2010.

680  
681  
682  
683

684 **Author contribution**

685 Na Zhao and Yabing He collected field samples, and performed the experiment. Na Zhao engaged in  
686 data analysis and writing this paper. Ping Meng proposed the suggestions on the theory and practice of  
687 experiment. Xinxiao Yu revised the paper and contributed to edit the manuscript.

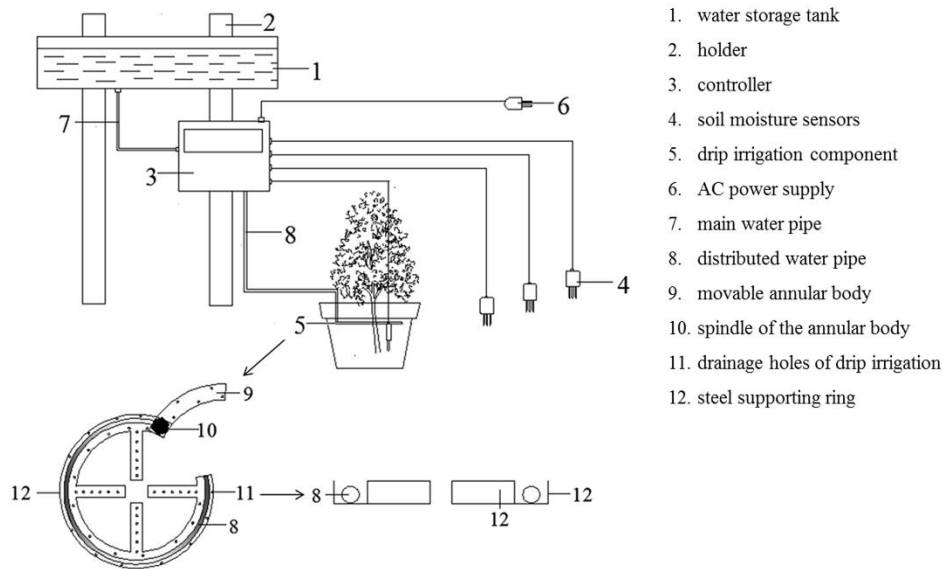
688

689 *Acknowledgements.* We would like to thank Beibei Zhou and Yuanhai Lou for kind **supports** in the  
690 collection of materials and management of saplings. We are grateful to anonymous reviewers for  
691 constructive suggestions of this manuscript. Due to the limitation of space allowed, we cited a part of  
692 literatures involving this study area and apologized for authors whose work has not been cited. All  
693 authors acknowledges support of National Natural Science Foundation of China (grant No. 41430747).

694  
695  
696  
697  
698  
699  
700  
701  
702  
703  
704  
705  
706  
707  
708  
709  
710  
711  
712  
713

714

## Figure



715

716 **Figure 1.** Structural diagram of the device for automatic drip irrigation

717 Arabic numerals indicate the individual parts of the automatic drip irrigation device (No. 1–7). The  
718 lower-left corner of this figure presents the detailed schematic for the drip irrigation components (No.  
719 8–12). The lower-right corner of this figure shows the schematic for the drip irrigation component in  
720 profile.

721

722

723

724

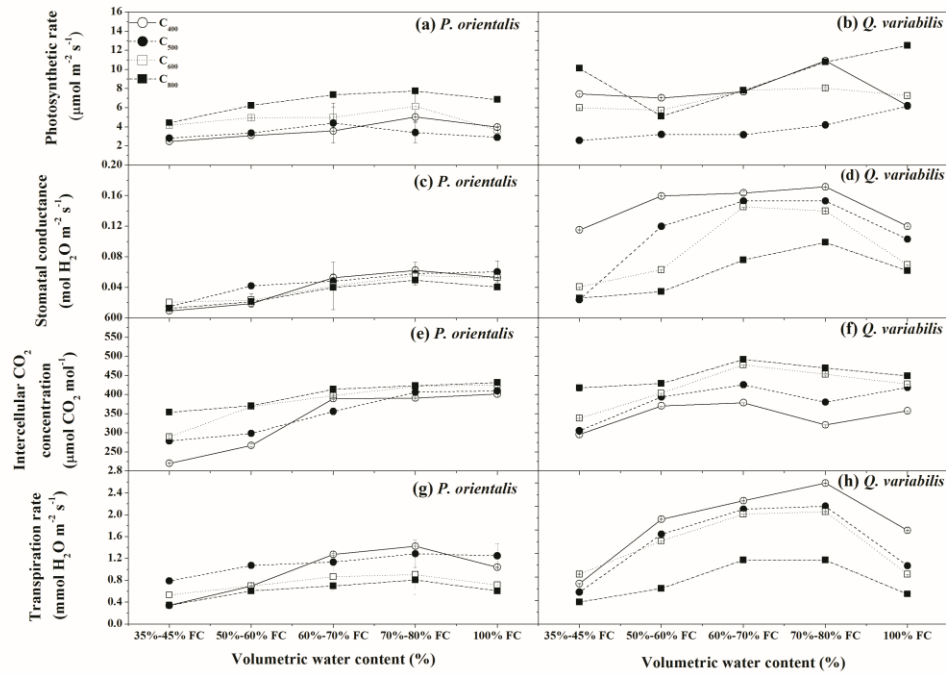
725

726

727

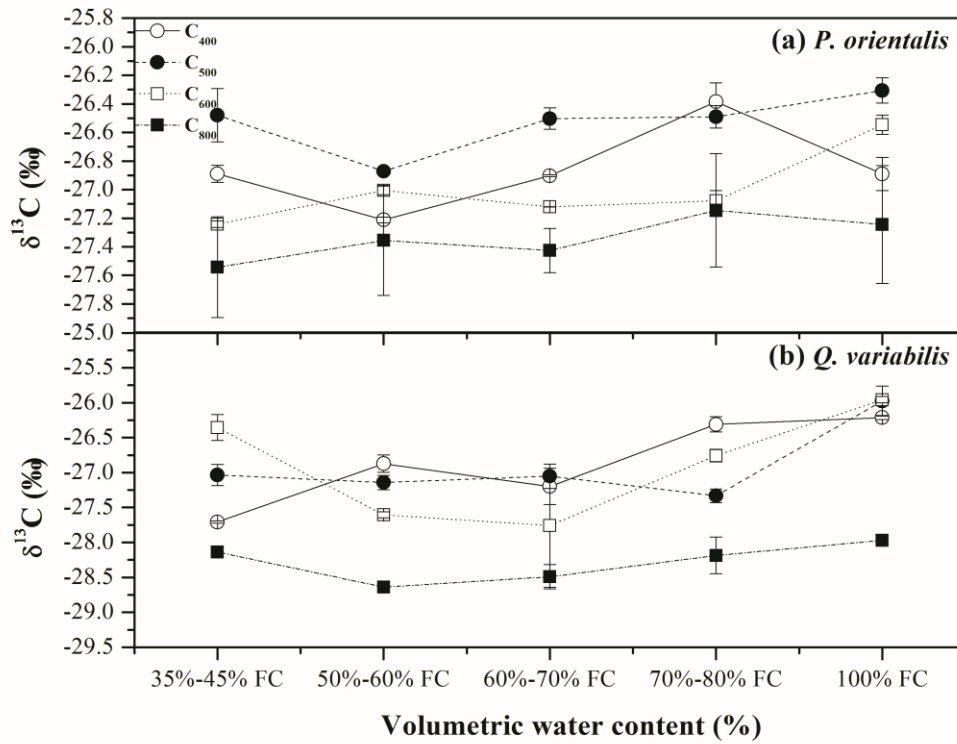
728

729



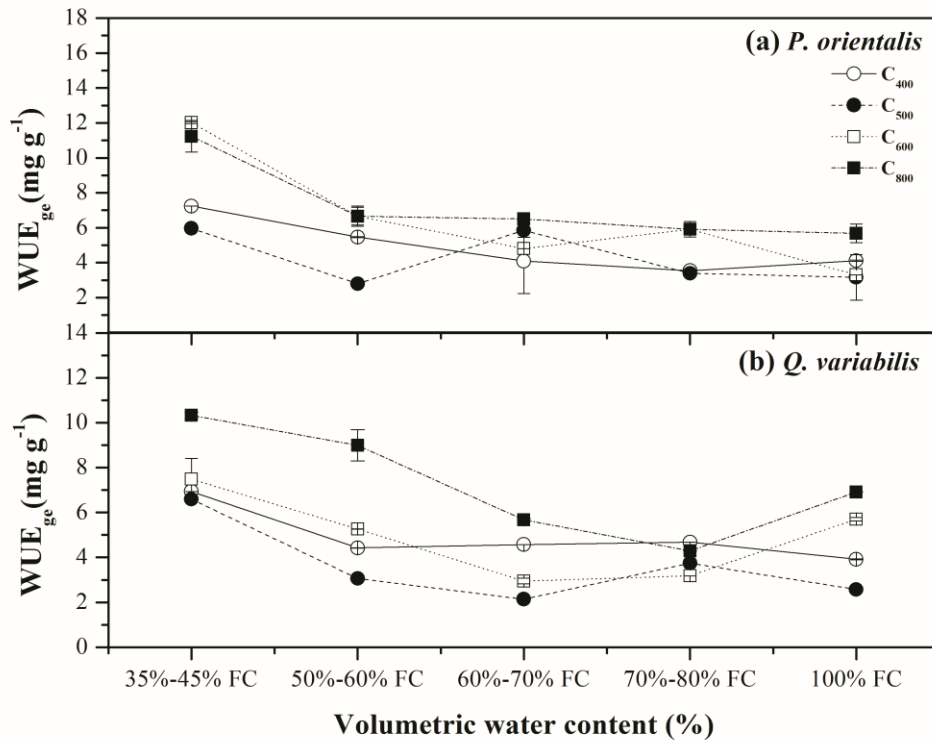
730

731 **Figure 2.** Photosynthetic parameters of *P. orientalis* and *Q. variabilis* saplings in CO<sub>2</sub> concentrations of  
 732 400 ppm, 500 ppm, 600 ppm and 800 ppm across five soil volumetric water contents. The net  
 733 photosynthetic rates ( $P_n$ ,  $\mu\text{mol m}^{-2} \text{s}^{-1}$ ), stomatal conductance ( $g_s$ ,  $\text{mol H}_2\text{O m}^{-2} \text{s}^{-1}$ ), intercellular CO<sub>2</sub>  
 734 concentration ( $C_i$ ,  $\mu\text{mol CO}_2 \text{mol}^{-1}$ ), and transpiration rates ( $T_r$ ,  $\text{mmol H}_2\text{O m}^{-2} \text{s}^{-1}$ ) are shown in Figs.  
 735 2a and 2b, 2c and 2d, 2e and 2g, and 2g and 2h, respectively. Means  $\pm$ SDs, n = 32.



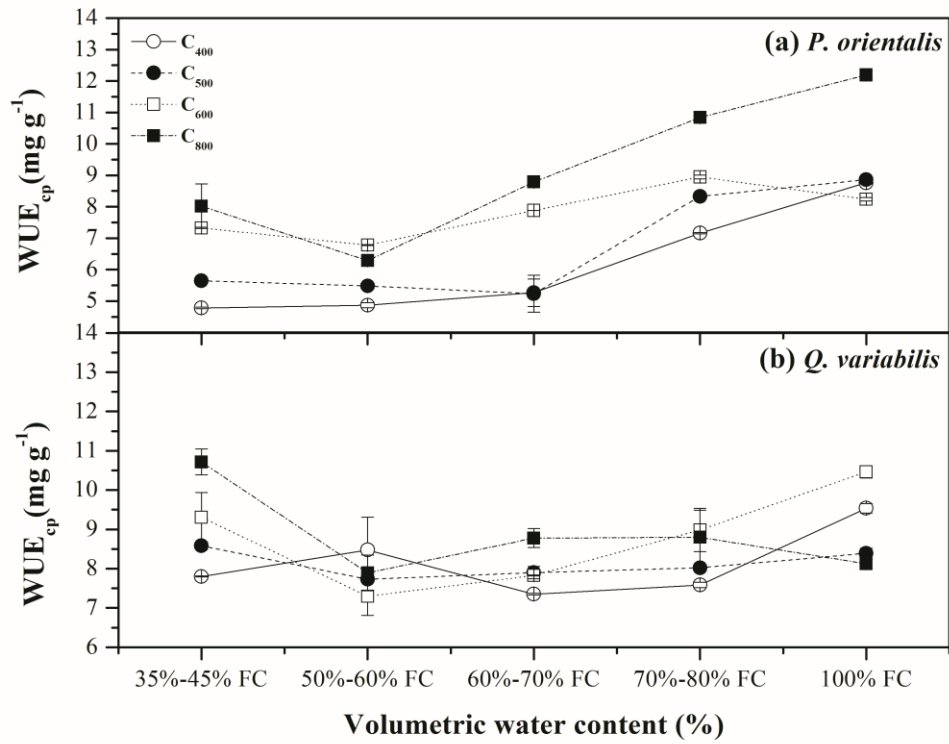
736

737 **Figure 3.**  $\delta^{13}\text{C}$  of water-soluble compounds extracted from leaves of *P. orientalis* and *Q. variabilis*  
 738 cultivated in CO<sub>2</sub> concentrations of 400 ppm, 500 ppm, 600 ppm and 800 ppm across five soil  
 739 volumetric water contents are shown in Figs. 3a and 3b. Means  $\pm$ SDs, n = 32.



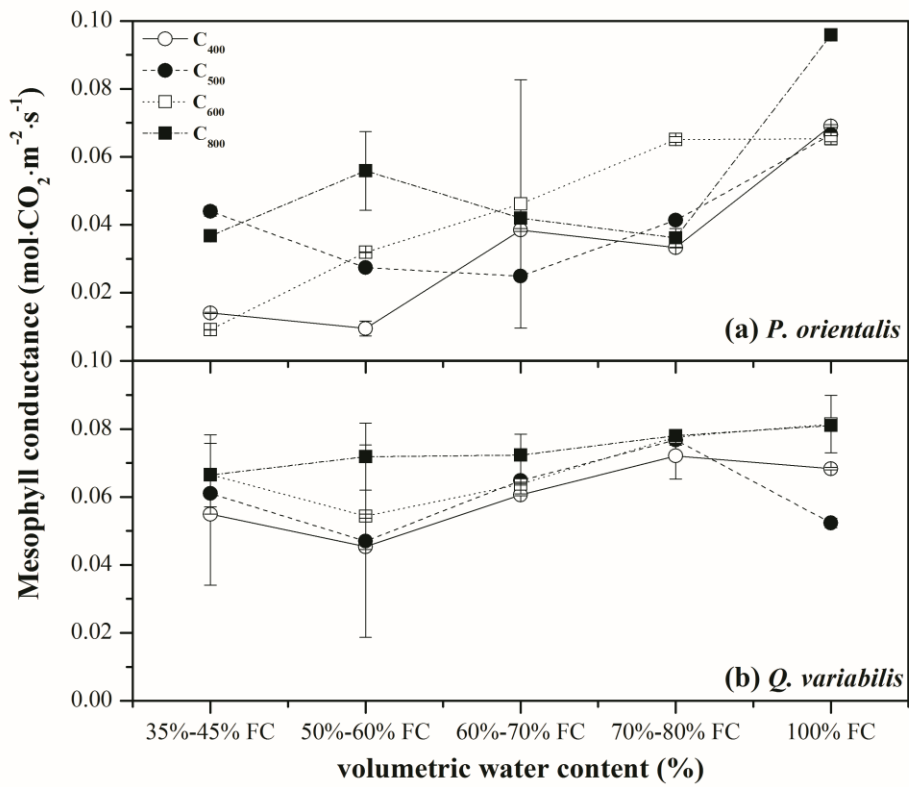
740

741 **Figure 4.** Instantaneous water use efficiency through gas exchange ( $WUE_{ge}$ ) in leaves of *P. orientalis*  
 742 and *Q. variabilis* cultivated in  $CO_2$  concentrations of 400 ppm, 500 ppm, 600 ppm and 800 ppm across  
 743 five soil volumetric water contents are shown in Figs. 4a and 4b. Means  $\pm$  SDs, n = 32.



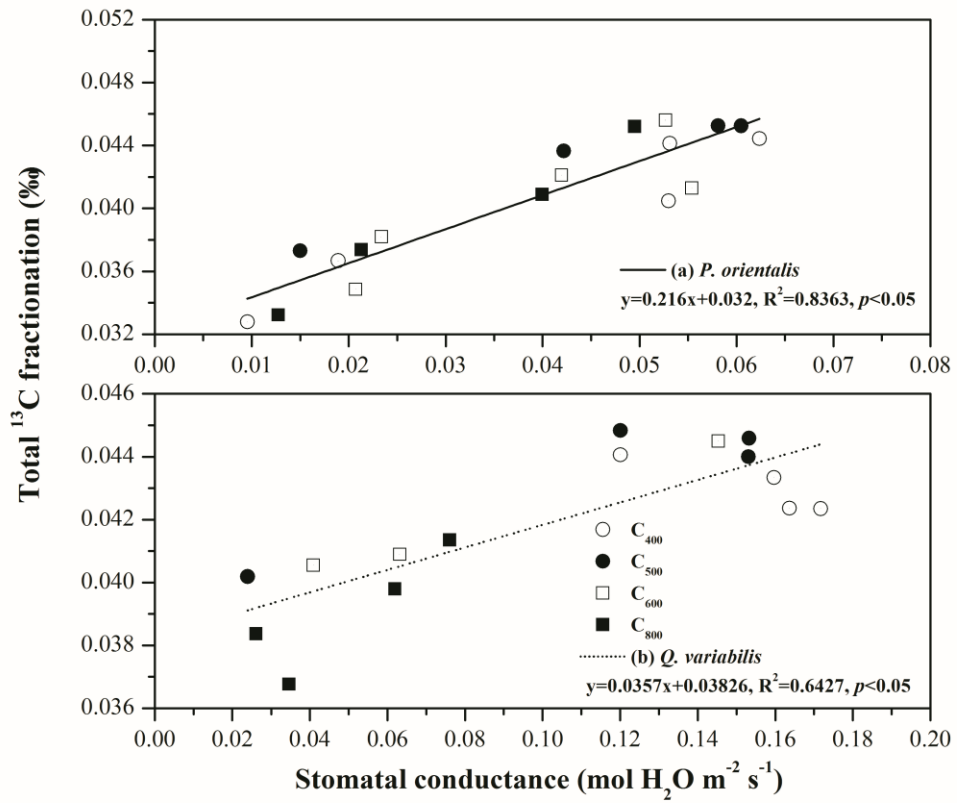
744

745 **Figure 5.** Instantaneous water use efficiency through  $\delta^{13}\text{C}$  of water-soluble compounds (WUE<sub>cp</sub>) in  
 746 leaves of *P. orientalis* and *Q. variabilis* cultivated in CO<sub>2</sub> concentrations of 400 ppm, 500 ppm, 600  
 747 ppm, and 800 ppm across five soil volumetric water contents are shown in Figs. 5a and 5b. Means  $\pm$   
 748 SDs, n = 32.



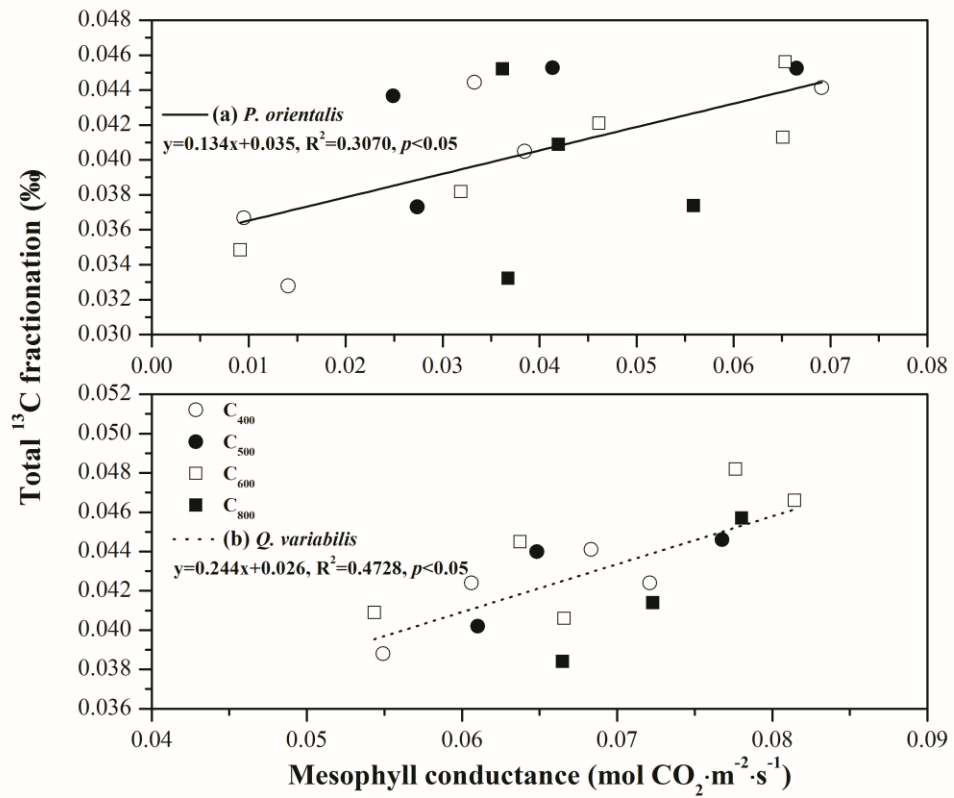
749

750 **Figure 6.** Variations in mesophyll conductance of *P. orientalis* and *Q. variabilis* cultivated in CO<sub>2</sub>  
 751 concentrations of 400 ppm, 500 ppm, 600 ppm, and 800 ppm across five soil volumetric water contents  
 752 are shown in Figs. 6a and 6b. Means ±SDs, n = 32.



753

754 **Figure 7.** Regression between stomatal conductance and total <sup>13</sup>C fractionation of *P. orientalis* and *Q.*  
 755 *variabilis* under four CO<sub>2</sub> concentrations × five soil volumetric water contents are established in Figs.  
 756 7a and 7b.  $p=0.05$ ,  $n = 32$ .



757

758 **Figure 8.** Regression between mesophyll conductance and total  $^{13}\text{C}$  fractionation of *P. orientalis* and *Q.*  
 759 *variabilis* under four  $\text{CO}_2$  concentrations  $\times$  five soil volumetric water contents are established in Figs.  
 760 8a and 8b.  $p=0.05$ ,  $n = 32$ .

761

**Table**762 **Table 1.**  $^{13}\text{C}$  fractionation of *P. orientalis* and *Q. variabilis* under four  $\text{CO}_2$  concentrations  $\times$  five soil volumetric water contents.

Species	SWC (of FC)	$\text{CO}_2$ concentration (ppm)													
		$^{13}\text{C}$				$^{13}\text{C}$									
		400	500	600	800	fractionation (‰)	400	500	600	800	fractionation (‰)	400	500	600	800
<i>P. orientalis</i>	35%–45%	0.0328	0.0373	0.0349	0.0332		0.0081	0.0030	0.0034	0.0072		0.0247	0.0343	0.0315	0.0260
	50%–60%	0.0367	0.0437	0.0382	0.0374		0.0018	0.0058	0.0094	0.0004		0.0349	0.0379	0.0288	0.0370
	60%–70%	0.0405	0.0366	0.0421	0.0409		0.0018	0.0050	0.0026	0.0007		0.0387	0.0316	0.0395	0.0402
	70%–80%	0.0444	0.0453	0.0413	0.0452		0.0044	0.0052	0.0103	0.0013		0.0400	0.0401	0.0310	0.0439
	100%	Total $^{13}\text{C}$ fractionation (‰)	0.0441	0.0453	0.0456	0.0472	Mesophyll conductance	0.0057	0.0040	0.0025	0.0039	Post- photosynthesis	0.0384	0.0413	0.0431
<i>Q. variabilis</i>	35%–45%	0.0388	0.0402	0.0406	0.0384		0.0007	0.0025	0.0006	0.0091		0.0381	0.0377	0.0400	0.0293
	50%–60%	0.0433	0.0448	0.0409	0.0368		0.0061	0.0084	0.0023	0.0018		0.0372	0.0364	0.0386	0.0350
	60%–70%	0.0424	0.0440	0.0445	0.0414		0.0066	0.0086	0.0078	0.0041		0.0358	0.0354	0.0367	0.0373
	70%–80%	0.0424	0.0446	0.0482	0.0457		0.0034	0.0016	0.0074	0.0028		0.0390	0.0430	0.0408	0.0429
	100%		0.0441	0.0466	0.0466	0.0398		0.0027	0.0076	0.0022	0.0125		0.0414	0.0390	0.0444

763